Combined high-pressure experimental and kinetic modeling study of cyclopentene pyrolysis and its reactions with acetylene

Alaa Hamadi, Leticia Carneiro Piton, Said Abid, Nabiha Chaumeix, Andrea Comandini

Available online at www.sciencedirect.com
ScienceDirect
Proceedings of the Combustion Institute 000 (2022) 1–10
Proceedings of the Combustion Institute
www.elsevier.com/locate/proci

Combined high-pressure experimental and kinetic modeling study of cyclopentene pyrolysis and its reactions with acetylene

Alaa Hamadi [a,1], Leticia Carneiro Piton [a,1], Said Abid [a,b], Nabiha Chaumeix [a], Andrea Comandini [a,*]

[a] *CNRS-INSIS, I.C.A.R.E., 1C, Avenue de la recherche scientifique, 45071 Orléans cedex 2, France*
[b] *Université d'Orléans, 6 Avenue du Parc Floral, 45100 Orléans, France*

Received 5 January 2022; accepted 3 July 2022
Available online xxx

Abstract

A combined experimental and kinetic modeling study is presented to improve the understanding of the formation of polycyclic aromatic hydrocarbons (PAHs) from neat cyclopentene and cyclopentene/acetylene mixtures. High-pressure experiments are conducted for the first time over a temperature range covering 930–1650 K using a single-pulse shock tube coupled to gas chromatography/gas chromatography-mass spectrometry (GC/GC–MS) techniques. Several updates and inclusions, mainly regarding the reactions involving C_5 molecules and radicals, are made in our on-going PAH kinetic model, which shows satisfactory predictive performances for the speciation measurements obtained in the current work and in the literature. On the basis of the experimental observations and modeling analyses, the reaction pathways active during the pyrolysis of cyclopentene are illustrated and the effects of acetylene addition as co-reactant on the PAH chemistry are assessed. In all of the cases investigated, it is noted that the cyclopentadienyl radical largely participate in the formation of mono-aromatic hydrocarbons (benzene and styrene) and PAHs (indene, naphthalene and phenanthrene).

Keywords: Cyclopentene; Acetylene; Pyrolysis; Single-pulse shock tube; Polycyclic aromatic hydrocarbons (PAHs)

1. Introduction

Interest in cyclopentene (CYC_5H_8) originates from its role as precursor of key C_5 intermediates, including cyclopentadiene (C_5H_6), whose chemistry strongly affects the formation of polycyclic hydrocarbons (PAHs) and soot. For instance, the ad-

* Corresponding author.
E-mail address: andrea.comandini@cnrs-orleans.fr (A. Comandini).
[1] The authors have contributed equally to the work.

https://doi.org/10.1016/j.proci.2022.07.023

dition of cyclopentene to n-heptane flames showed potential to modify the soot properties by favoring curvature in the carbonaceous structures [1]. More in general, at typical flame temperatures, C_5H_6 is easily converted into cyclopentadienyl radical (C_5H_5), an important intermediate for the formation of high amounts of mono-aromatics (MAHs) and PAHs [2–4]. Recent research shows that PAHs can be produced via the recombination reactions of C_5H_5 radicals [5–8], and chain addition reactions of C_5H_5 with the methyl radical [9–12], acetylene [13,14], or ethylene [15]. Therefore, the experimental and kinetic modeling study on CYC_5H_8 pyrolysis at high-pressure conditions typically encountered in combustion devices is crucial in order to improve our understanding of the molecular weight growth processes involving C_5 species.

Nevertheless, only two kinetic studies focused on the pyrolysis of cyclopentene are available in the literature. King [16] measured the kinetic parameters of cyclopentene thermal decomposition reaction into 1,3-cyclopentadiene and hydrogen. More recently, Herbinet et al. [17] performed atmospheric-pressure pyrolysis experiments in a jet-stirred reactor in the temperature range covering 773–1048 K. Products up to naphthalene were measured using three complementary analytical methods, and a kinetic model was proposed.

In this contribution, single-pulse shock tube pyrolysis experiments of highly diluted mixtures containing 108 ppm and 326 ppm cyclopentene are carried out at a nominal pressure of 20 bar over a temperature range between 940 K and 1650 K. In addition, to investigate the effects of acetylene addition, co-pyrolysis experiments of 111 ppm cyclopentene + 517 ppm acetylene are performed. Based on the newly obtained species profiles up to three-ring products, the sub-mechanism of cyclopentene is updated in our on-going kinetic model for PAH chemistry [18]. The combined experimental observations and kinetic modeling interpretations provide answers for major questions regarding: 1. the thermal decomposition of cyclopentene and its main products; 2. the influence of reactions involving the cyclopentadienyl radical on the formation of mono- and poly-aromatic species; 3. the effects of acetylene on cyclopentene reactivity and PAH speciation.

2. Shock tube pyrolysis experiments

The pyrolysis experiments are carried out with the high-purity single-pulse shock tube facility at ICARE, Orléans. The detailed description of the set-up and the experimental procedures is well documented in our previous publications, i.e. [18,19]. Briefly, the shock tube is composed of a 78-mm inner diameter and 6-m long driven section, and a 120-mm inner diameter and 3.7-m long driver section. Both sections are separated by a double diaphragm. A 150 L dump tank is attached to the driven section near the diaphragm for operation in a single-pulse fashion. The driven section is heated to 90 °C to reduce condensation or absorption of heavy species and it is pumped down below 10^{-5} mbar before each experiment. The inner surface of the driven section is cleaned daily to remove carbon deposits.

Four pressure sensors (CHIMIE METAL A25L05B), mounted on the sidewall at the end part of the driven section, record the time of the shock wave passage for the calculation of the incident shock velocity, which is further used to determine the post-shock conditions T_5 and p_5 by solving the conservation equations together with the ideal gas law and variable heat capacity ratio. The maximum uncertainty in the calculated T_5 is within ±30 K, mainly due to the wave attenuation and to the uncertainty in the determination of the actual positions of the pressure sensor sensitive surfaces. Such spatial uncertainties are estimated in a conservative way to be 2 mm, equal to the sensor diameter. A PCB Piezotronics pressure sensor, shielded by a layer of room-temperature vulcanizing (RTV) silicone, is mounted on the end-wall and it is used to record the pressure time-history for each shock from which the corresponding reaction time can be defined [20]. A typical end-wall pressure profile is shown in Fig. S1 in the Supplementary Material. The reaction time is ∼ 4 ms in the current experimental configuration.

The post-shock gas products are sampled with an air-actuated valve and they are analyzed using an Agilent 7890B gas chromatograph (GC) and a Thermo Trace GC/DSQ mass spectrometer. The Agilent GC is equipped with a flame ionization detector (FID) detector and a thermal conductivity detector (TCD) connected respectively to a DB-17 ms column for measurement of heavy species and to a Molseive 5A column for measurement of inert compounds and for verifying the absence of air. The Thermo Trace GC is equipped with an FID detector connected to an HP Plot Q column for measuring light species up to mono-aromatics. Standard gas mixtures, delivered by Air Liquide, are used for the calibration of light C_1-C_5 hydrocarbons except for diacetylene (C_4H_2) and triacetylene (C_6H_2) for which the calibration factors are obtained from high-temperature acetylene (C_2H_2) pyrolysis experiments through carbon atom conservation. The liquid fuels, including benzene, toluene, styrene and phenylacetylene, are calibrated with mixtures prepared in stainless steel vessels by the partial pressure method. On the other hand, for small PAHs up to three rings, the calibrations are performed with gas-phase mixtures prepared in a heated glass vessel (200 °C) to minimize the surface absorption [21], and the detailed procedure is explained in [22]. Likewise, the 1,3-cyclopentadiene calibration mixture is obtained by heating dicyclopentadiene above its boiling point before dilu-

Please cite this article as: A. Hamadi, L.C. Piton, S. Abid et al., Combined high-pressure experimental and kinetic modeling study of cyclopentene pyrolysis and its reactions with acetylene, Proceedings of the Combustion Institute, https://doi.org/10.1016/j.proci.2022.07.023

Table 1
Compositions of the gas mixtures used in this study.

Mixture	CYC_5H_8	C_2H_2	Impurities
Neat CYC_5H_8	108 ppm	—	C_5H_6: 0.2 ppm, LC_5H_8: 0.45 ppm
Neat CYC_5H_8	326 ppm	—	C_5H_6: 1.2 ppm, LC_5H_8: 1.9 ppm
$CYC_5H_8 + C_2H_2$	111 ppm	517 ppm	C_5H_6: 0.2 ppm, LC_5H_8: 0.45 ppm, CH_4: 1.7 ppm

tion with argon. The uncertainty in the measurements is expected to be within 5% for directly calibrated small species, and 10%−15% for PAH species calibrated in gas phase. These uncertainties derive from the reproducibility of the single measure when repeated several times and the uncertainties in the composition of the initial reference calibration mixtures which reflects in the accuracy of the calibration curves.

Concerning the chemicals used in the experiments, cyclopentene (96%) is provided by Sigma-Aldrich. Other gases, including acetylene (C_2H_2) (>99.5%) and argon (>99.9999%), are supplied by Air-Liquide. A 450B Matheson gas purifier with a 454 cartridge is connected to the acetylene bottle to remove the possible acetone traces, and acetone is found to be below the detection limit of the GC system in all the experiments (less than 0.1 ppm). The experimental gas mixtures are prepared in 136 L electropolished stainless steel cylinder at least 12 h before use to ensure good homogeneity. The exact compositions of the experimental mixtures are listed in Table 1.

3. Kinetic modeling

The current work is a continuation of our previous serial works towards building a comprehensive kinetic model capable to predict the pyrolytic PAH formation at high-pressure and temperature conditions [18]. Since the latest CRECK PAH model by Pejpichestakul et al. [23] was selected as the starting point of our model development [19], the C_5 sub-mechanism is already included in the core mechanism of the on-going kinetic model. Only the updated and added reactions are mentioned here. The unimolecular decomposition reactions of cyclopentene to pentadiene and C_5H_6 as well as the H- addition to allene (C_3H_6) are updated from the model by Dayma et al. [24]. The unimolecular decomposition of C_5H_6 can generate allene/propyne (C_3H_4-A/C_3H_4-P)+C_2H_2. Their rate constants are taken from POLIMI_1311 model [25]. The combination reaction between C_5H_5 and C_2H_2 can produce the heptatrienyl radical (cC_7H_7), and then cC_7H_7 can react with another C_2H_2 to form indene. The corresponding rate constants are taken from the theoretical calculations from da Silva et al. [13] and Fascella et al. [14], respectively. The recombination reaction of C_5H_5 + propargyl (C_3H_3) producing styrene is added from the model by Yuan et al. [26]. The pathway to produce indene (C_9H_8) through the addition of C_5H_5 to C_5H_6 is adopted from Vervust et al. [15]. Long et al. [8] recalculated the potential energy surface of C_5H_5 self-recombination which involves numerous C_{10} intermediates and their reactions. The pressure-dependent rate constants of these reactions are included in the current model. The rate coefficient for the reaction between indenyl and C_5H_5 forming phenanthrene is from the work by Herbinet et al. [17].

The thermochemical data for most species is from the latest version of CRECK model [23] since it is the basis of the current model [19]. For the species introduced by reactions added or updated in the present work, their thermochemical data originate from the same publication from which the reaction rate constant parameters were taken.

Simulations presented in the discussion are performed with the homogeneous reactor model of the COSILAB software [27] using a constant p_5 of 20 bar and a nominal reaction time of 4 ms. The constant pressure assumption is well justified [20,28], and well applies to our experimental configuration. Nevertheless, simulations with T_5 at the zero time point and measured pressure profiles up to 10 ms are sometimes necessary, as they take into account the reactions that occur in the quenching period, particularly those involving resonantly stabilized radicals such as cyclopentadienyl [29,30]. The simulations with the measured pressure profiles up to 10 ms are shown in Figs. S2-S4 in the Supplementary Material. Both methods give similar predictions except for acenaphthylene (as discussed later). Recent kinetic mechanisms developed by Herbinet et al. [17] and Vervust et al. [15] are also used to simulate the current experiments for comparison purposes. It is important to underline that the model by Vervust et al. [15] is developed for the co-pyrolysis of C_5H_6 and ethene, and it is also validated against cyclopentadiene pyrolysis data in flow reactors, including PAH formation chemistry up to naphthalene. Since in the case of CYC_5H_8 pyrolysis the PAH chemistry of the second-ring is mainly driven by the C_5H_6 chemistry, the model is here used for further validation of the pathways to naphthalene. The impurities, addressed in Table 1, are considered in the simulations, but their presence does not significantly affect the simulation results.

The present kinetic model was also tested against the literature data on the pyrolysis of cyclopentene and cyclopentadiene in jet stirred re-

Please cite this article as: A. Hamadi, L.C. Piton, S. Abid et al., Combined high-pressure experimental and kinetic modeling study of cyclopentene pyrolysis and its reactions with acetylene, Proceedings of the Combustion Institute, https://doi.org/10.1016/j.proci.2022.07.023

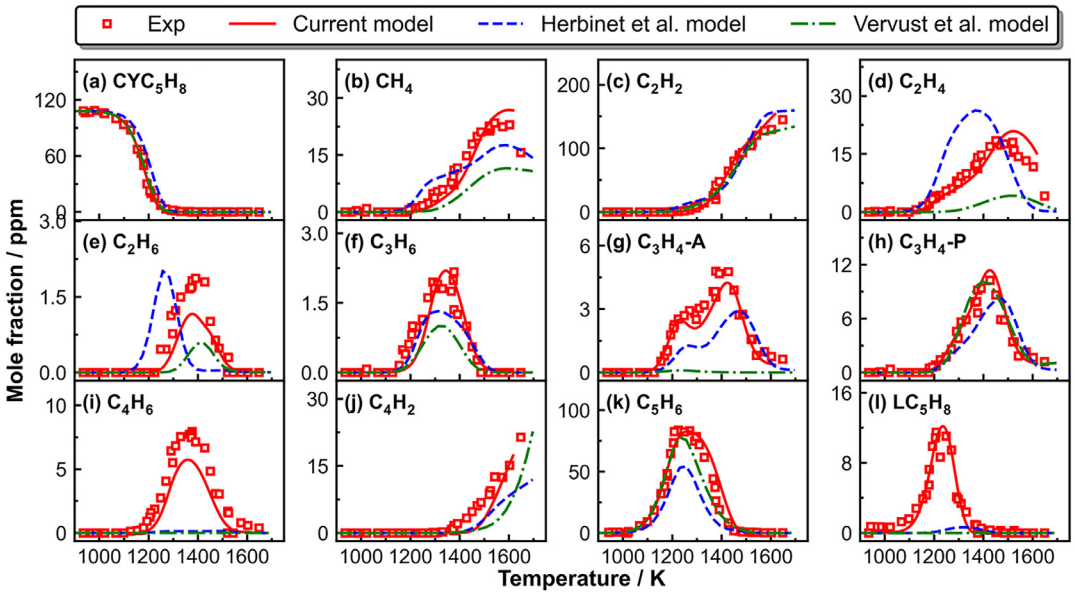

Fig. 1. Measured (symbols) and simulated (lines) profiles of fuel and the C_0–C_5 species as a function of T_5 in 108 ppm cyclopentene pyrolysis. Thick solid red lines: simulations using the current kinetic model; thin dashed blue lines: simulations using the Herbinet et al. [17] model; thin dot dashed green lines: simulations using the Vervust et al. [15] model.

actors and flow reactors (Figs. S5-S8). The model does a reasonably good job in reproducing all the data at different conditions, especially in relation to the formation of PAHs. Finally, the comparison between the current kinetic model and the original CRECK model is presented in Figs. S2-S4. A considerable improvement of the performances was achieved particularly in relation with the prediction of the PAH profiles.

4. Results and discussion

In this section, the first step is to examine the CYC_5H_8 decomposition reactivity and the speciation of small intermediates, and then put emphasis on the production of aromatic species, from the simplest benzene to larger PAHs. Only the data from 108 ppm CYC_5H_8 pyrolysis are presented in the discussion, while the ones for 326 ppm are given in Figs. S9-S10 in the Supplementary Material. The second step is to reveal the influences of added C_2H_2 on the speciation patterns of CYC_5H_8 pyrolysis, with particular attention paid to the PAH formation pathways. To this end, the species pools and the reaction schemes of CYC_5H_8+C_2H_2 pyrolysis are compared with those of neat CYC_5H_8 pyrolysis.

4.1. Fuel decomposition and the formation of small hydrocarbons

Fig. 1 (and Fig. S9 for the set with 326 ppm initial fuel mole fraction) shows the mole fraction profiles of the fuel and the C_0-C_5 species as a function of T_5, including measurements and simulations using the current model and the different kinetic models from the literature.

The current model satisfactorily captures the fuel reactivity and the formation of the major products with respect to both the temperature windows and the peak concentrations. According to the integrated rate-of production (ROP) analyses, CYC_5H_8 is consumed mainly through dehydrogenation and ring-opening isomerization reactions leading to the formation of C_5H_6 and LC_5H_8, respectively (CYC_5H_8=C_5H_6+H_2: 84% and CYC_5H_8=LC_5H_8: 11% throughout the conversion range). Direct evidences of these reactions cover two aspects: i) C_5H_6 and LC_5H_8 formation temperature windows overlap with the fuel decomposition; and ii) C_5H_6 and LC_5H_8 mole fractions coincide with percentage consumption of CYC_5H_8 throughout their formation windows. It is noteworthy to point out here that LC_5H_8 is lumped in the current model and it is the sum of 1,4-pentadiene and 1,3-pentadiene isomers.

Small hydrocarbons are formed directly from the fuel reactions with H atoms, the C_5 intermediates consumption pathways, or through subsequent reactions of the small fragmentation products. The consumption of LC_5H_8 leads mainly to the formation of 1,3-butadiene (C_4H_6) and propene (C_3H_6) [31]. C_4H_6 is predominantly formed through the H-addition reaction to LC_5H_8 (H+LC_5H_8=C_4H_6+methyl (CH_3)). C_3H_6 is mainly produced through the reaction

Please cite this article as: A. Hamadi, L.C. Piton, S. Abid et al., Combined high-pressure experimental and kinetic modeling study of cyclopentene pyrolysis and its reactions with acetylene, Proceedings of the Combustion Institute, https://doi.org/10.1016/j.proci.2022.07.023

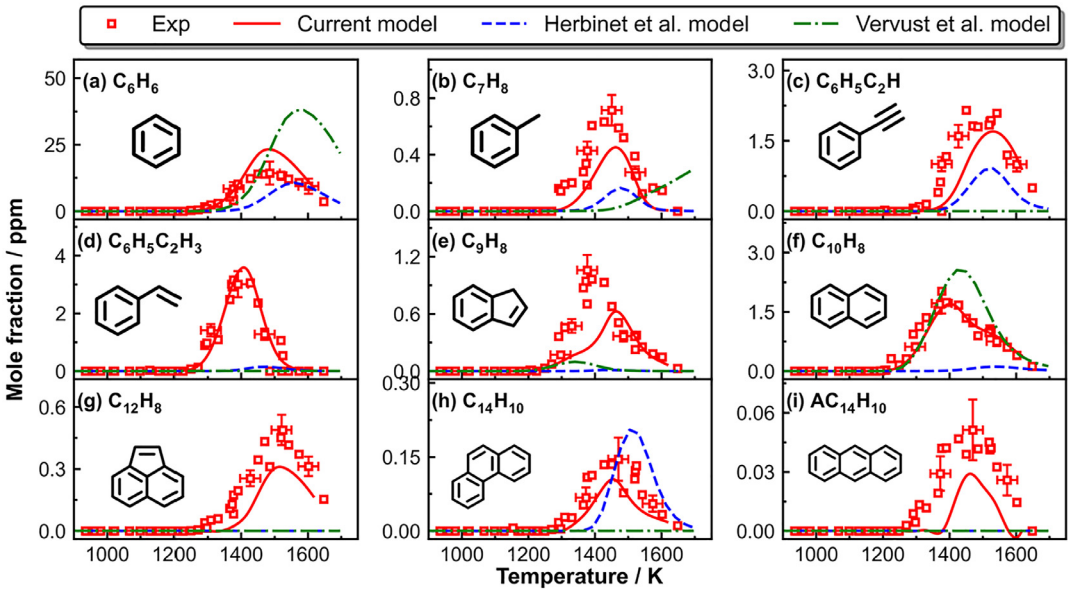

Fig. 2. Measured (symbols) and simulated (lines) mole fraction profiles of the aromatic species as a function of T_5 in 108 ppm cyclopentene pyrolysis. Thick solid re d lines: simulations using the current kinetic model; thin dashed blue lines: simulations using the Herbinet et al. [17] model; thin dot dashed green lines: simulations using the Vervust et al. [15] model.

LC_5H_8=C_2H_2+C_3H_6, and minorly through H+LC_5H_8=C_3H_6+vinyl (C_2H_3). The dehydrogenation process of allyl (C_3H_5-A), which comes from C_3H_6, and H-addition to CYC_5H_8/LC_5H_8 (H+CYC_5H_8/LC_5H_8=C_3H_5-A+C_2H_4), is the prevailing pathway leading to allene (C_3H_4-A) formation at low temperatures (around 1200 K). The C_5H_6 unimolecular decomposition into C_2H_2+C_3H_4-A also slightly contributes to C_3H_4-A (6% at 1250 K). At higher temperatures, these pathways have comparable contribution (55% for the former one and 41% for the latter one at 1400 K). The consumption of C_3H_4-A largely leads to the formation of propyne (C_3H_4-P) through isomerization. Another important pathway for C_3H_4-P formation is through C_5H_6 unimolecular decomposition into C_2H_2+C_3H_4-P. The consumption of C_3 fuels, namely propene and propyne, and C_4H_6 through H-abstraction reactions leads to the production of CH_3. The H+CH_3 recombination reaction and the hydrogen abstraction reactions by CH_3 from C_5H_6 give rise to the formation of methane (CH_4). Ethane (C_2H_6) is exclusively produced from the self-recombination of CH_3. The C_2H_6 consumption subsequently contributes to C_2H_4 production. Other important pathways for C_2H_4 formation include the H-addition reactions to CYC_5H_8 (H+CYC_5H_8=C_3H_5-A+C_2H_4), LC_5H_8 (H+LC_5H_8= C_3H_5-A+C_2H_4), C_4H_6 (H+C_4H_6=C_2H_3+C_2H_4), and C_3H_6 (H+C_3H_6=CH_3+C_2H_4). There are numerous formation pathways for C_2H_2. Most of C_2H_2 comes from C_5H_5 unimolecular decomposition (C_5H_5=C_2H_2+C_3H_3), C_2H_3 unimolecular decomposition (C_2H_3=C_2H_2+H), the C_5H_6 decomposition (C_5H_6=C_2H_2+C_3H_4-P), and the H-atom addition fragmentation of C_3H_4-P (H+C_3H_4-P= C_2H_2+ CH_3). The consumption of both C_4H_6 and C_2H_4 yields vinyl radical.

The kinetic model by Herbinet et al. [17] slightly underpredicts the reactivity of the fuel but it captures the formation of the main intermediates such as acetylene, C_3 fuels, and cyclopentadiene (although with slight under-prediction). Larger discrepancies can be seen for C_2H_4, C_2H_6 and CH_4, as well as for C_4H_6 and linear C_5H_8 whose production is not predicted. On the other hand, the model by Vervust et al. [15] perfectly captures the reactivity of the fuel as well as the initial formation and peak concentration of cyclopentadiene, thus it can be used to further test the pathways involving the cyclic C_5 + cyclic C_5 reaction pathways to naphthalene.

4.2. Aromatic formation

Fig. 2 (Fig. S10 for the set with 326 ppm initial fuel mole fraction) presents the mole fraction profiles of MAHs and PAHs as a function of T_5. The current model can well reproduce the speciation profiles regarding the temperature windows and the peak concentrations. The aromatic formation pathways, based on integrated ROP analyses at T_5=1400 K, where most aromatics have considerable concentrations, are displayed in Fig. 3. The shown pathways start from C_5H_5 that is formed

Please cite this article as: A. Hamadi, L.C. Piton, S. Abid et al., Combined high-pressure experimental and kinetic modeling study of cyclopentene pyrolysis and its reactions with acetylene, Proceedings of the Combustion Institute, https://doi.org/10.1016/j.proci.2022.07.023

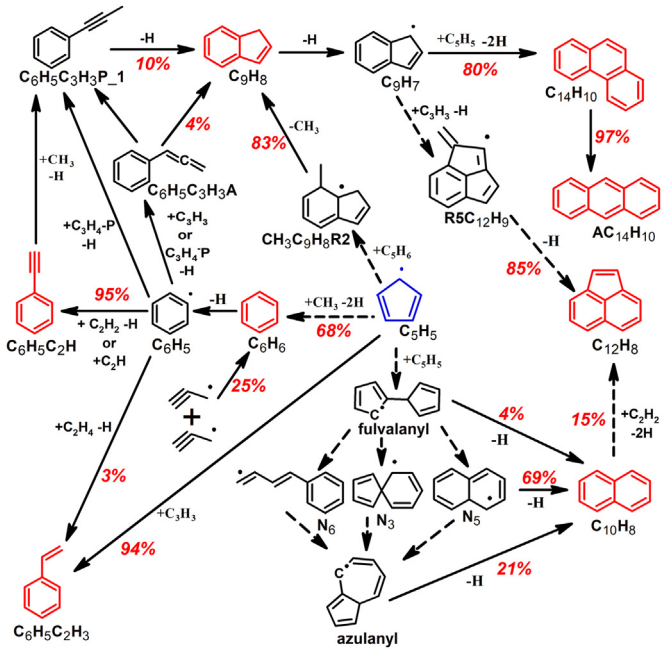

Fig. 3. The reaction pathways leading to aromatics formation based on integrated ROP analyses at T_5 of 1400 K in the pyrolysis of 108 ppm CYC_5H_8. The percentage numbers represent the contributions of the corresponding reactions to the formation of the species. The dashed arrows resemble multi-step reactions.

through H-abstraction reactions from C_5H_6, the most abundant product in CYC_5H_8 pyrolysis (Fig. 1).

The reaction of C_5H_5 with small species leads to the formation of various MAHs including benzene (C_6H_6), toluene (C_7H_8), styrene ($C_6H_5C_2H_3$), and phenylacetylene ($C_6H_5C_2H$). The C_5H_5 recombination with CH_3 followed by hydrogen elimination results in three C_6H_7 isomers ($C_5H_5CH_2$–1, $C_5H_5CH_2$–2, and $C_5H_4CH_3$), which further undergo C–C beta scission for ring expansion and a C–H beta scission to give C_6H_6 and H atom. Another important benzene formation pathway is through propargyl recombination (Fig. 3). C_7H_8 is mainly formed through the recombination reactions of propargyl with C_4H_6 and but–2-yn-1-yl radical ($\dot{C}H_2C{\equiv}CCH_3$), respectively. The formation of C_7H_8 through C_5H_6+C_2H_2 reaction is only 5% at 1400 K. The limited toluene production through this channel and the under-predication of the model to C_7H_8 peak mole fraction in both sets (Fig. 2(b) and Fig. S10 (b)) suggest that either more theoretical work on C_5H_6+C_2H_2 is needed or formation channels are missing. $C_6H_5C_2H_3$ is predominantly produced through C_5H_5+C_3H_3 reactions, and slightly through C_6H_5+C_2H_4 reaction. $C_6H_5C_2H$ is totally formed through phenyl (C_6H_5) +C_2H_2/C_2H reactions.

C_5H_5 also is involved in the formation of PAHs, including naphthalene ($C_{10}H_8$) and indene (C_9H_8), the most abundant ones detected in the current study. In particular, the C_5H_5+C_5H_5 recombination reaction results in fulvalane isomers, which decompose into fulvalanyl radicals. Fulvalanyl radicals lead to $C_{10}H_8$ through a progressive isomerization process [8], and this reaction sequence is the principal source of $C_{10}H_8$ formation in cyclopentene pyrolysis, according to the modeling analyses (Fig. 3). Indene is mainly formed through the addition of C_5H_5 to C_5H_6 through the intermediate methylindanyl ($CH_3C_9H_8R2$) [15]. The modeling analysis shows that the kinetic parameters of the first step (addition of C_5H_5 to C_5H_6) are very sensitive under the conditions of the present study. This pathway merits future investigations through theoretical calculations, which would be valuable for improving indene formation. Another sequence of reactions starting with the addition of the phenyl radical to propyne/propargyl contributes in a lower extent to indene formation. Following the formation of indene, indenyl plays an important role in aromatic growth. Indeed, the interactions of indenyl with propargyl and C_5H_5 dominate the formation of acenaphthylene ($C_{12}H_8$) and phenanthrene ($PC_{14}H_{10}$), respectively. The HACA pathway through naphthyl ($C_{10}H_7$)+C_2H_2 and bibenzyl dehydrogenation ([32], not shown) also contribute around 15% and 18% in $C_{12}H_8$ and $PC_{14}H_{10}$ formation, respectively. 15% of $C_{12}H_8$ is formed during the post-shock quenching, mainly through the

Please cite this article as: A. Hamadi, L.C. Piton, S. Abid et al., Combined high-pressure experimental and kinetic modeling study of cyclopentene pyrolysis and its reactions with acetylene, Proceedings of the Combustion Institute, https://doi.org/10.1016/j.proci.2022.07.023

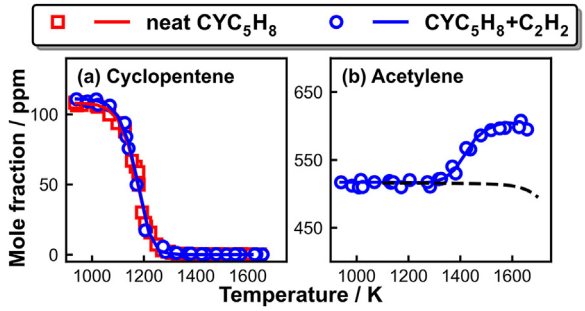

Fig. 4. Experimental (symbols) and simulated (solid lines) mole fractions of (a) CYC_5H_8 in the two investigated cases, (b) C_2H_2 in the pyrolysis of 111 ppm CYC_5H_8 + 526 ppm C_2H_2 mixture. The dashed line in (b) represents the simulated mole fractions of C_2H_2 when CYC_5H_8 is absent from the corresponding mixture.

C_9H_7+C_3H_3 recombination [22], as shown in Figs. S2 and S3). Anthracene ($AC_{14}H_{10}$) is totally formed from phenanthrene isomerization. Based on the above discussion, the cyclopenta-ring species are further proved as important precursors leading to the formation and growth of aromatic rings.

The models from the literature do not provide an accurate description of the experimental profiles of the mono- and poly-aromatics. On the other hand, we can notice how the formation of naphthalene is well captured by the model by Vervust et al. [15]. As this model is capable to reproduce the cyclopentadiene mole fractions (Fig. 1), this result further supports the accuracy of the reactions and related kinetic parameters involving two cyclic C_5 compounds and leading to the formation of the second-ring structure.

4.3. Influence of C_2H_2 addition on cyclopentene consumption and small intermediates

First, the influence of the abundant C_2H_2 on CYC_5H_8 decomposition reactivity is inspected. Fig. 4 displays the fuel concentrations as a function of the post-shock temperature T_5 in neat cyclopentene and cyclopentene+C_2H_2 pyrolysis. The kinetic model satisfactorily predicts the measured fuel conversion profiles in the studied cases. As observed from Fig. 4, both the experimental and the modeling results indicate that C_2H_2 addition has no influence on CYC_5H_8 reactivity. C_2H_2 remains unreactive at temperatures below 1250 K. To better illustrate the mutual effects between the binary fuel components, the simulated profile of neat C_2H_2 is also shown in Fig. 4(b) as a reference. C_2H_2 starts forming at temperatures above 1300 K due to its production from the yielded small intermediates in CYC_5H_8 decomposition (refer to Section 4.1).

Concerning the small hydrocarbons, they are qualitatively and quantitatively similar to the ones in neat CYC_5H_8 as well as their formation pathways (Fig. S11). However, the addition of acetylene slightly enhances the formation of propyne and allene at high temperatures through the reaction CH_3+C_2H_2=C_3H_4-p/C_3H_4-A +H (Fig. S11 (f) and (g)). This reaction pathway impedes the CH_3 self-recombination reaction leading to a decrease in C_2H_6 peak mole fraction (Fig. S11 (d)). Moreover, the presence of C_2H_2 in the initial mixture contributes in the build-up of the C_4H_2 mole fraction (Fig. S11 (j)) at elevated temperatures due to the increased number of carbon atoms.

4.4. Impacts of acetylene addition on aromatics formation

One major purpose of this work is to illustrate the impacts of C_2H_2 on aromatics speciation in CYC_5H_8 pyrolysis. Quantitative measurements of the aromatic products and their corresponding simulations are presented in Fig. 5. Overall, the current kinetic model can satisfactorily reproduce the shown concentration profiles within the experimental uncertainties. The two experimental data sets show no obvious differences in the onset temperature and the peak mole fractions of C_6H_6 (Fig. 5(a)) and $C_6H_5C_2H_3$ (Fig. 5(d)). Thus, the extra C_2H_2 has no influence on C_6H_6 and $C_6H_5C_2H_3$ formation as they are mainly formed through C_5H_5+CH_3 and C_5H_5+C_3H_3, respectively. The addition of C_2H_2 to CYC_5H_8 amplifies the concentrations of $C_6H_5C_2H$ (Fig. 5(c)) and 1-ethynylnaphthalene ($C_{10}H_7C_2H$, (Fig. 5(h)). Indeed, the formation of $C_6H_5C_2H$ and $C_{10}H_7C_2H$ largely depends on the C_6H_5/$C_{10}H_7$+ C_2H_2 reactions, and the presence of C_2H_2 in the initial mixture facilitates their production. C_7H_8 starts forming at relatively lower temperature in CYC_5H_8/C_2H_2 co-pyrolysis (Fig. 5(b)). Indeed, the carbon flux into C_7H_8 through C_5H_6+ C_2H_2 recombination is increased from 5% in neat cyclopentene to 40% at T_5 = 1400 K.

Regarding other major PAHs, the presence of C_2H_2 in the initial mixture enhances the peak mole fraction of indene, and it has more pronounced effect in the simulated results in comparison to experiments. In neat CYC_5H_8, C_9H_8 formation is

Please cite this article as: A. Hamadi, L.C. Piton, S. Abid et al., Combined high-pressure experimental and kinetic modeling study of cyclopentene pyrolysis and its reactions with acetylene, Proceedings of the Combustion Institute, https://doi.org/10.1016/j.proci.2022.07.023

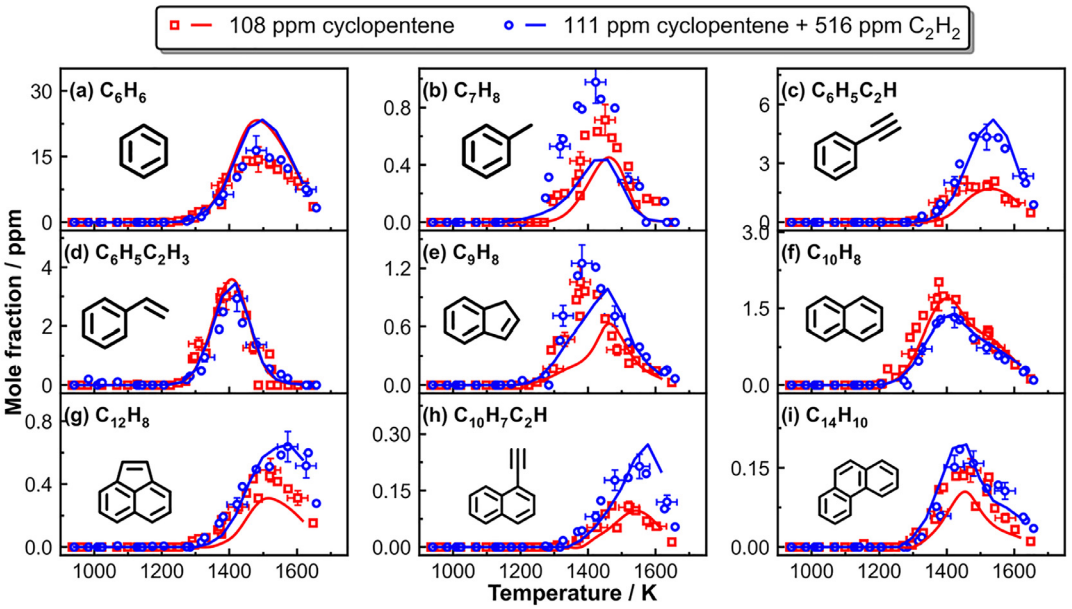

Fig. 5. Measured (symbols) and simulated (lines) mole fraction profiles of aromatics in the pyrolysis of 108 ppm cyclopentene and 111 ppm cyclopentene+ 517 ppm acetylene.

governed by C_5H_5+C_5H_6 reaction. However, in CYC_5H_8+C_2H_2 co-pyrolysis, a newly introduced channel is found to play a vital role in C_9H_8 formation through the reaction sequence starting from C_5H_5+C_2H_2 proposed by da Silva et al. [13] and Fascella et al. [14]. The enhanced indene formation in the binary mixture clearly increases the peak concentrations of acenaphthylene and phenanthrene, as they mainly originate from reactions involving indenyl. Compared to case of neat cyclopentene pyrolysis, the presence of C_2H_2 slightly impedes the formation of naphthalene owing to the fact that the predominant reaction sequence through C_5H_5 self-recombination is hindered by the lowered C_5H_5 level (Fig. S12 in the Supplementary Material) as a small part of C_5H_5 reacts with C_2H_2.

5. Conclusion

The pyrolysis of cyclopentene with and without the presence of acetylene was studied in a single-pulse shock tube coupled to GC/GC–MS techniques under highly argon-diluted conditions with the goal of providing new experimental insights on PAH formation from cyclic C_5 species. Species profiles were obtained over the temperature range covering 930–1650 K at a nominal pressure of 20 bar and a nominal reaction time of 4 ms. With updates in reactions involving C_5 species, our on-going kinetic model emphasizing PAH chemistry could well interpret how cyclopentene is consumed under high-pressure pyrolytic conditions, and how the resulting intermediates react to form PAHs, and furthermore, how the extra acetylene impacts the reaction schemes. In all the investigated cases, cyclopentene mainly decomposes into linear pentadienes and cyclopentadiene. Their consumption mainly contributes to the formation of small hydrocarbons and cyclopentadienyl radical (C_5H_5), respectively. C_5H_5 either decomposes to form small molecules, or reacts with other species, including methyl, propargyl, cyclopentadiene and cyclopentadienyl radical itself leading to the formation of benzene, styrene, indene and naphthalene, respectively. The subsequent reactions of indenyl radical with propargyl and cyclopentadienyl radicals are essential pathways leading to acenaphthylene and phenanthrene, respectively. When extra C_2H_2 is introduced to the reaction system, cyclopentene decomposition reactivity is not influenced, but the PAH speciation is slightly altered. The main pathway for the formation of indene shifts to C_5H_5 + C_2H_2, which inhibits C_5H_5 self-recombination leading to a decrease in the naphthalene peak. Increases are also seen in the mole fractions of the aromatic species whose formation depends on the reactions involving acetylene, namely phenylacetylene and ethynyl naphthalene. In the presence of acetylene, toluene formation is initiated at lower temperatures by acetylene addition to cyclopentadiene. Furthermore, the current model well predicts the trends of all major and minor products reported in literature studies, and considerably outperforms established models in the literature when simulated against our data.

Please cite this article as: A. Hamadi, L.C. Piton, S. Abid et al., Combined high-pressure experimental and kinetic modeling study of cyclopentene pyrolysis and its reactions with acetylene, Proceedings of the Combustion Institute, https://doi.org/10.1016/j.proci.2022.07.023

Declaration of Competing Interest

The authors declare that they have no known competing financial interests or personal relationships that could have appeared to influence the work reported in this paper.

Acknowledgements

This project has received funding from the European Research Council (ERC) under the European Union's Horizon 2020 research and innovation programme (grant agreement no. 756785).

Supplementary materials

Supplementary material associated with this article can be found, in the online version, at doi:10.1016/j.proci.2022.07.023.

References

[1] M. Salamanca, M. Botero, J. Martin, J. Dreyer, J. Akroyd, M. Kraft, The impact of cyclic fuels on the formation and structure of soot, Combust. Flame 219 (2020) 1–12.
[2] M.R. Djokic, K.M. Van Geem, C. Cavallotti, A. Frassoldati, E. Ranzi, G.B. Marin, An experimental and kinetic modeling study of cyclopentadiene pyrolysis: first growth of polycyclic aromatic hydrocarbons, Combust. Flame 161 (2014) 2739–2751.
[3] D.H. Kim, J.A. Mulholland, D. Wang, A. Violi, Pyrolytic hydrocarbon growth from cyclopentadiene, J. Phys. Chem. A 114 (2010) 12411–12416.
[4] R.G. Butler, I. Glassman, Cyclopentadiene combustion in a plug flow reactor near 1150K, Proc. Combust. Inst. 32 (2009) 395–402.
[5] V.V. Kislov, A.M. Mebel, The formation of naphthalene, azulene, and fulvalene from cyclic C5 species in combustion: an ab initio/RRKM study of 9-H–fulvalenyl (C5H5−C5H4) radical rearrangements, J. Phys. Chem. A. 111 (2007) 9532–9543.
[6] A.M. Mebel, V.V. Kislov, Can the C5H5 + C5H5 → C10H10 → C10H9 + H/C10H8 + H2 reaction produce naphthalene? An ab initio/RRKM study, J. Phys. Chem. A 113 (2009) 9825–9833.
[7] C. Cavallotti, D. Polino, On the kinetics of the C5H5+C5H5 reaction, Proc. Combust. Inst. 34 (2013) 557–564.
[8] A.E. Long, S.S. Merchant, A.G. Vandeputte, H.-.H. Carstensen, A.J. Vervust, G.B. Marin, K.M. Van Geem, W.H. Green, Pressure dependent kinetic analysis of pathways to naphthalene from cyclopentadienyl recombination, Combust. Flame 187 (2018) 247–256.
[9] C. Cavallotti, S. Mancarella, R. Rota, S. Carrà, Conversion of C5 into C6 cyclic species through the formation of C7 intermediates, J. Phys. Chem. A 111 (2007) 3959–3969.
[10] S. Sharma, W.H. Green, Computed rate coefficients and product yields for c-C5H5 + CH3 –>products, J. Phys. Chem. A 113 (2009) 8871–8882.
[11] K. Wang, S.M. Villano, A.M. Dean, Reactions of allylic radicals that impact molecular weight growth kinetics, Phys. Chem. Chem. Phys. 17 (2015) 6255–6273.
[12] V.S. Krasnoukhov, D.P. Porfiriev, I.P. Zavershinskiy, V.N. Azyazov, A.M. Mebel, Kinetics of the CH3 + C5H5 reaction: a theoretical study, J. Phys. Chem. A 121 (2017) 9191–9200.
[13] G. da Silva, J.A. Cole, J.W. Bozzelli, Kinetics of the cyclopentadienyl + acetylene, fulvenallene + H, and 1-ethynylcyclopentadiene + H reactions, J. Phys. Chem. A 114 (2010) 2275–2283.
[14] S. Fascella, C. Cavallotti, R. Rota, S. Carrà, The peculiar kinetics of the reaction between acetylene and the cyclopentadienyl radical, J. Phys. Chem. A 109 (2005) 7546–7557.
[15] A.J. Vervust, M.R. Djokic, S.S. Merchant, H.-.H. Carstensen, A.E. Long, G.B. Marin, W.H. Green, K.M. Van Geem, Detailed experimental and kinetic modeling study of cyclopentadiene pyrolysis in the presence of ethene, Energy Fuels 32 (2018) 3920–3934.
[16] K. King, Very low-pressure pyrolysis (VLPP) of cyclopentene, Int. J. Chem. Kinet. 10 (1978) 117–123.
[17] O. Herbinet, A. Rodriguez, B. Husson, F. Battin-Leclerc, Z. Wang, Z. Cheng, F. Qi, Study of the formation of the first aromatic rings in the pyrolysis of cyclopentene, J. Phys. Chem. A 120 (2016) 668–682.
[18] A. Hamadi, W. Sun, S. Abid, N. Chaumeix, A. Comandini, An experimental and kinetic modeling study of benzene pyrolysis with C2−C3 unsaturated hydrocarbons, Combust. Flame 237 (2022) 111858.
[19] W. Sun, A. Hamadi, S. Abid, N. Chaumeix, A. Comandini, Probing PAH formation chemical kinetics from benzene and toluene pyrolysis in a single-pulse shock tube, Proc. Combust. Inst. 38 (2021) 891–900.
[20] W. Tang, K. Brezinsky, Chemical kinetic simulations behind reflected shock waves, Int. J. Chem. Kinet. 38 (2006) 75–97.
[21] A. Comandini, T. Malewicki, K. Brezinsky, Online and offline experimental techniques for polycyclic aromatic hydrocarbons recovery and measurement, Rev. Sci. Instrum. 83 (2012) 034101.
[22] W. Sun, A. Hamadi, S. Abid, N. Chaumeix, A. Comandini, A comprehensive kinetic study on the speciation from propylene and propyne pyrolysis in a single-pulse shock tube, Combust. Flame 231 (2021) 111485.
[23] W. Pejpichestakul, E. Ranzi, M. Pelucchi, A. Frassoldati, A. Cuoci, A. Parente, T. Faravelli, Examination of a soot model in premixed laminar flames at fuel-rich conditions, Proc. Combust. Inst. 37 (2019) 1013–1021.
[24] G. Dayma, S. Thion, Z. Serinyel, P. Dagaut, Experimental and kinetic modelling study of the oxidation of cyclopentane and methylcyclopentane at atmospheric pressure, Int. J. Chem. Kinet. (2020).
[25] E. Ranzi, A. Frassoldati, R. Grana, A. Cuoci, T. Faravelli, A.P. Kelley, C.K. Law, Hierarchical and comparative kinetic modeling of laminar flame speeds of hydrocarbon and oxygenated fuels, Prog. Energy Combust. Sci. 38 (2012) 468–501.
[26] W. Yuan, Y. Li, P. Dagaut, J. Yang, F. Qi, Experimental and kinetic modeling study of styrene combustion, Combust. Flame 162 (2015) 1868–1883.
[27] COSILABThe Combustion Simulation Laboratory, Rotexo GmbH & Co., KG, Haan, Germany, 2009 Version 3.3.2, (n.d..

Please cite this article as: A. Hamadi, L.C. Piton, S. Abid et al., Combined high-pressure experimental and kinetic modeling study of cyclopentene pyrolysis and its reactions with acetylene, Proceedings of the Combustion Institute, https://doi.org/10.1016/j.proci.2022.07.023

[28] X. Han, J.M. Mehta, K. Brezinsky, Temperature approximations in chemical kinetics studies using single pulse shock tubes, Combust. Flame 209 (2019) 1–12.
[29] J.A. Manion, D.A. Sheen, I.A. Awan, Evaluated kinetics of the reactions of H and CH3 with n-alkanes: experiments with n-butane and a combustion model reaction network analysis, J. Phys. Chem. A 119 (2015) 7637–7658.
[30] L.A. Mertens, I.A. Awan, D.A. Sheen, J.A. Manion, Evaluated site-specific rate constants for reaction of isobutane with H and CH3: shock tube experiments combined with bayesian model optimization, J. Phys. Chem. A 122 (2018) 9518–9541.
[31] K. Wang, S.M. Villano, A.M. Dean, Fundamentally-based kinetic model for propene pyrolysis, Combust. Flame 162 (2015) 4456–4470.
[32] S. Sinha, A. Raj, Polycyclic aromatic hydrocarbon (PAH) formation from benzyl radicals: a reaction kinetics study, Phys. Chem. Chem. Phys. 18 (2016) 8120–8131.

Please cite this article as: A. Hamadi, L.C. Piton, S. Abid et al., Combined high-pressure experimental and kinetic modeling study of cyclopentene pyrolysis and its reactions with acetylene, Proceedings of the Combustion Institute, https://doi.org/10.1016/j.proci.2022.07.023